*32nd EPS Conference on Plasma Phys. Tarragona, 27 June - 1 July 2005 ECA Vol.**29C**, P-5.053 (2005)*

Transport properties and magnetic fluctuations in RFX-mod

L.Marrelli, A.Alfier, F.Bonomo, A.Cravotta,, P.Franz, M.Gobbin,P. Innocente, P.Martin, E.Martines, P.Nielsen, R.Pasqualotto, P.Piovesan, I.Predebon, G.Serianni, G.Spizzo, D.Terranova, P.Zanca
Consorzio RFX - Associazione EURATOM ENEA sulla FUSIONE, Padova, Italy

The modified RFX (RFX-mod) reversed field pinch (RFP) device, that recently resumed operations, is a unique facility to study the physics of RFP plasmas with a thin shell [1], and the effect of magnetic fluctuations on transport. This is made possible both by the particular MHD dynamics of the RFP configuration and by the advanced diagnostic capabilities of the device. The influence of magnetic fluctuations on transport in the RFP is, in fact, linked both to their amplitude, and to the structure of their spatial spectrum. Spectra dominated by one m=1 dynamo mode, as those predicted in the single helicity (SH) regime, are expected to have a much reduced impact on transport [2]. Experimental measurements show indeed that in quasi-SH regime dynamo might have a more laminar character [3]. While average properties of magnetic fluctuations spectra are described elsewhere [4], we focus here on the thermal properties and of the observations of quasi-SH in the first RFX-mod experimental campaign. Experiments aimed at a preliminary investigation of low to intermediate current regimes ($0.2 < I_p < 0.65$ MA), with electron density varied in the range $1\ 10^{19}\ m^{-3} < n_e < 6\ 10^{19}\ m^{-3}$. In particular, different startup scenarios for 400 kA discharges have been compared [1].

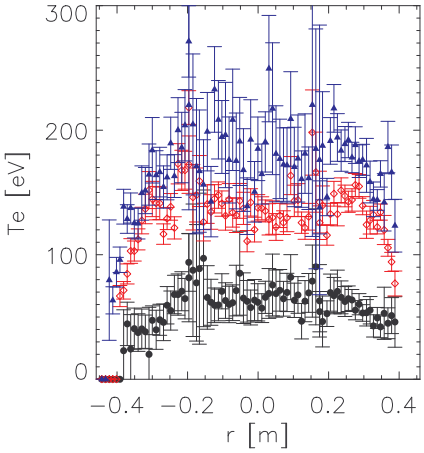

Fig. 1) Electron temperature profiles for 0.2 (black), 0.4(red),and 0.6(blue) MA.

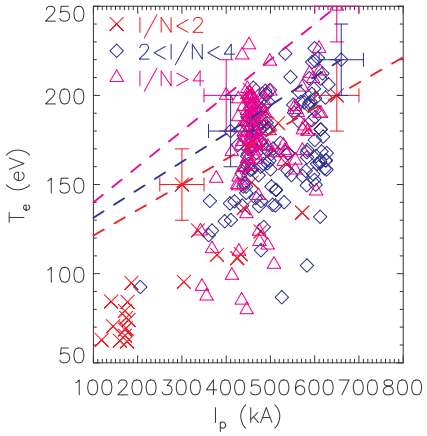

Fig. 2) On-axis T_e vs I_p, for three different values of the I/N parameter

Electron temperature. An enhanced spatial resolution Thomson scattering diagnostic is now in operation: the diagnostic measures the entire Te profile along a diameter in the equatorial plane with 84 spatial positions, with a spatial resolution of 7 mm and a repetition rate of 25 ms. Principal features of the diagnostic are: a Nd:YAG laser which produces up to 10 pulses with E=4J, filter polychromators with APDs and waveform

digitizers.[5]. An example of Te(r) for three levels of plasma current is shown in Fig. 1. Further diagnostic optimizations are in progress in order to reduce systematic errors due to plasma emission in the spectral region around the laser wavelength. The on-axis temperature is estimated by averaging the measurements between -0.2m and 0.2m. The scaling of the temperature with plasma current for a range of values of the I/N parameter is shown in Fig. 2. The plasma regime is not optimized yet, therefore the electron temperatures of present RFX-mod experiments are below the optimized discharges of RFX (continuous lines) [6]. Still, normalized magnetic fluctuations are found to decrease (Fig. 3) with a parameter proportional to the Lundquist number $S \propto I_p\ Te(0)^{3/2}\ n_e^{-1/2}$ (i.e. the ratio between the resistive diffusion time and the Alfvén time; see [7] for the definition). The scaling law is consistent with RFX observations [7].

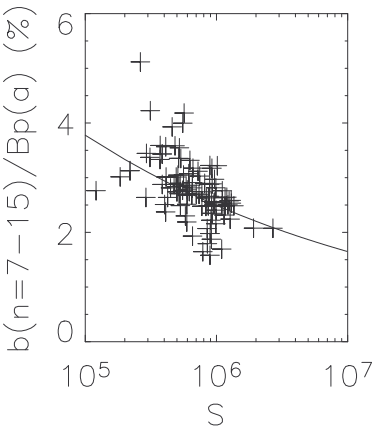

Fig. 3) Magnetic fluctuations amplitude vs. Lundquist number.

Statistical properties of magnetic perturbation spectra in RFX-mod: The toroidal magnetic field perturbation spectrum of a RFP is dominated by m=1 perturbations. Similarly to RFX [8], spectra in RFX-mod are typically dominated by an m=1 n=-8 or by an m=1 n=-7 both in 600 kA and in 400 kA discharges. Statistical properties of the magnetic spectrum during the plasma current flat-top (defined as the time interval in which the plasma current is at least 70% of its maximum value) have been analysed by considering a database of 1 ms averages of measurements at 3 ms intervals. Consistently with observations in other RFP experiments [9], the decrease of the width of the magnetic spectrum (measured by the spectral spread parameter $N_s = \left(\sum_{n=7,15}\left(b_n^2 / \sum_s b_s^2\right)\right)^{-1}$, where N_s=1 characterizes a pure Single Helicity spectrum) is due both to the increase of the amplitude of the dominant mode and to the decrease of the average amplitude of the secondary ones (see Fig. 4). The spectrum of the radial component is similar but typically the mode amplitudes increase in time due to the penetration time of the shell (as it may be observed, for example, in Fig. 5).

The magnetic spectrum during the plasma current flat-top seems to be influenced by the start-up phase of the discharge. During the initial exploration of the experimental parameter space, in fact, three different setting-up of the discharge were considered: aided-reversal, matched-reversal and ramping [1]. Within the limited number of the performed experiments, we observe that the ramping start-up is more often characterised by low values of the N_s parameter especially in the current ramp-up phase. If we consider N_s<3.5 as a definition of a QSH for RFX-mod, for the 400kA discharges the fraction of QSH intervals are 3%, 7% and 15% for aided, matched and ramping start-up, respectively.

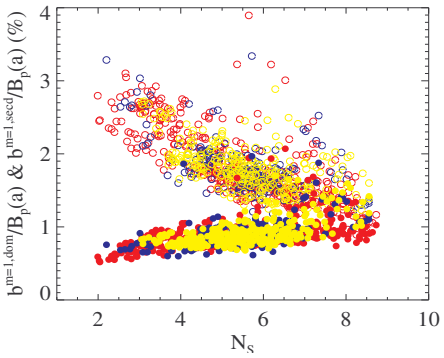

Fig. 4) Normalized amplitude of the dominant (open) and of the average of secondary (full) modes vs. Ns .Red) ramping, blue) aided, yellow) matched startup.

The details of the equilibrium determine the helicity of the dominant mode: different locations in the (F,θ) space are in fact characterized by an n=-8 or by an n =-7 dominant mode (see Fig. 6).

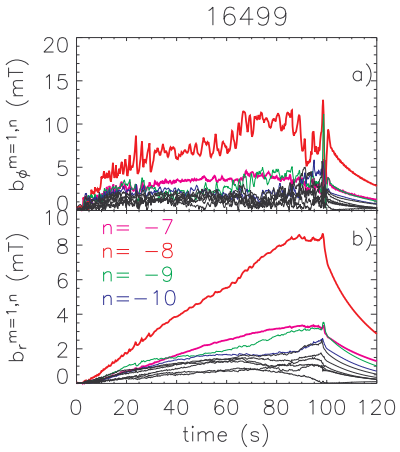

Fig. 5) a) toroidal, b) radial magnetic perturbationst, during a qsh discharge.

SXR structures: In 600 kA discharges SXR emissivity is measurable with a sufficient signal/noise ratio. In this regime, poloidally localized SXR structures are found during QSH regimes (Fig. 7-a). These structures are detected by the SXR tomographic diagnostic, which measures the line-integrated SXR emissivity through a 25 μm thick Beryllium filter, along 78 lines of sight arranged in 4 fans [10]. Poloidal harmonics up to m=2 can be reconstructed by adopting the Cormack approach with the Bessel functions radial base. The enhanced SXR emissivity regions correspond poloidally and radially with the magnetic islands appearing in Poincaré plots obtained with the ORBIT code [2], used to reconstruct the internal topology of the magnetic field lines. The code requires as input the equilibrium fields and the profile of the radial component of

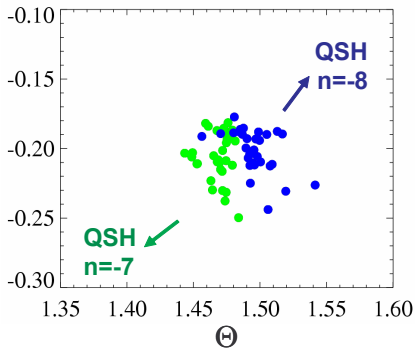

Fig. 6) F vs θ for a series of discharges with Ns < 3.5

the magnetic perturbations. While the former are obtained by numerically integrating a cylindrical force free equilibrium, the radial field profile is obtained by a solving the cylindrical Newcomb equation [11]. Measurements of both the toroidal and the radial component of the magnetic field at the edge are used as boundary conditions for the equation.

In the experiments performed up to now, the helical SXR structures appear and disappear intermittently, even when the dominant mode amplitude remains at relatively high level compared to secondary modes. The intermittent behavior can be correlated with the dynamics of the magnetic spectrum as detected by magnetic diagnostics. In the particular case shown here, a necessary condition for the SXR structure to appear is that the ratio between the n=-8 (i.e. the dominant mode) and the n=-9 exceeds a threshold value.

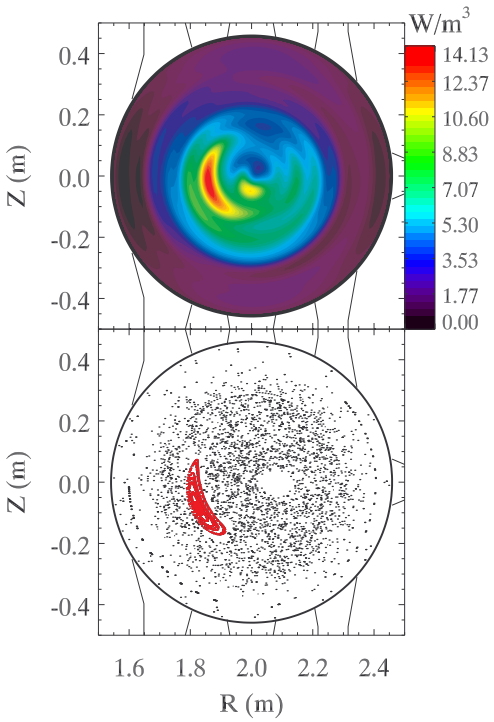

Fig. 7)a) SXR emissivity map and b) magnetic field line tracing for a magnetic island during a QSH period.

More experiments will be devoted in the future to investigations both on the spontaneous and on the actively controlled transition to QSH spectra, using the 192 saddle coils of the RFX-mod feedback system [12].

Acknowledgement. This work was supported by the European Communities under the contract of Association between EURATOM/ENEA. The views and opinions expressed herein do not necessarily reflect those of the European Commission.

---

1 S. Martini *et al*., this conference.
2 I. Predebon *et al*., *Phys. Rev. Lett*. **93** (2004) 145001
3 P.Piovesan *et al*. *Phys. Rev. Lett* **93** (2004)
4 T.Bolzonella *et al.*, this conference
5 R. Pasqualotto. P. Nielsen, L. Giudicotti, *Rev. Sci. Instrum*. **72** 1134 (2001)
6 R.Bartiromo *et al*., *Phys. Plas*. **6** (1999) 1830
7 A.Intravaia *et al.*, *Phys Rev.Lett.* **83** (1999) 5499;D.Terranova et al, *Plas.Phys.Contr.Fus.* **42** (2000) 843
8 D.F. Escande *et al.*, *Phys. Rev. Lett*. **85** (2000) 1662
9 P. Piovesan *et al.*, *Phys. Plas*. **11** (2004) 151
10 P.Franz *et al.*, *Nucl. Fus*. **41** (2001) 695
11 D. Terranova, P. Zanca, *Plas. Phys. Contr. Fus.* **46** (2004) 1115
12 P.Sonato et al, to be published in *Fus. Eng. Des.*